Jurnal Tribologi 49 (2026) 53-67

MYTRIBOS Malaysian Tribology Society

Jurnal Tribologi

Website : jurnaltribologi.mytribos.org e-issn: 2289-7232

Improvement of tribological properties of aluminium 7075 enhanced with TiO nanoparticles by friction stir processing

Muhammad Zulkarnain [1*], Lailatul Harina Paijan [2], Mohammad Kamil Sued [2], Abdul Munir Hidayat Syah Lubis [3]

[1] Faculty of Mechanical Technology and Engineering, Universiti Teknikal Malaysia Melaka, 76100 Durian Tunggal, Melaka, MALAYSIA.
[2] Faculty of Industrial and Manufacturing Technology and Engineering, Universiti Teknikal Malaysia Melaka, Hang Tuah Jaya, 76100 Durian Tunggal, Melaka, MALAYSIA.
[3] Department of Engineering, Higher Colleges of Technology, 0000 Abu Dhabi, UNITED ARAB EMIRATES.
*Corresponding author: m.zulkarnain@utem.edu.my

KEYWORDS

Friction stir process
Al7075
TiO_2
Tribology

ABSTRACT

The primary goal of this research is to enhance the surface properties of 7075 aluminium alloys using the friction stir process (FSP). The research investigates the effects of tool speed and traverse rate on the tribological properties of these alloys by incorporating titanium dioxide (TiO_2) nanoparticles as reinforcements. The study examined the impact of varying volume percentages (vol%: 4%, 8%, 12%) of TiO_2 within the aluminium matrix. The study adjusted the tool rotational speed (ω) to be fixed at 1300 rpm and the traverse speed (v) between 15 and 45 mm/min. Preliminary findings show that the lubrication provided by TiO_2 nanoparticles significantly enhances wear resistance, outperforming the hardening effects alone. This research aims to unlock new possibilities for improved performance in aluminium alloys across various applications. The optimal tribological performance was observed at tool rotational speeds of 1300 rpm, with traverse speeds of 45 mm/min and reinforcement volume fractions of 12%.

Received 25 July 2025; received in revised form 14 October 2025; accepted 22 October 2025.
To cite this article: Zulkarnain et al. (2026). Improvement of tribological properties of aluminium 7075 enhanced with TiO nanoparticles by friction stir processing. Jurnal Tribologi 49, pp.53-67.

1.0 INTRODUCTION

The demand for materials exhibiting high strength, stiffness, and low density has significantly increased across critical sectors such as automotive, aerospace, energy, and construction. Conventional monolithic materials often fail to meet the multifaceted performance requirements of these applications. Consequently, metal matrix composites (MMCs) have emerged as a promising class of engineered materials, combining metallic matrices with high-performance reinforcements to achieve superior mechanical and physical properties (Abbasi-Nahr et al., 2024; Rehman et al., 2012; Sidharthan et al., 2023). MMCs consist of a continuous metallic matrix—commonly based on Al, Mg, Ti, Cu, or Fe – and a dispersed reinforcement phase, typically ceramic particulates (e.g., Si, Ti, TiB_2) or fibers (e.g., carbon, glass, boron) (Beldar and Kadbhane, 2025; Liu et al., 2025; Prasad et al., 2024; Rehman et al., 2012; Roshan et al., 2024; Sidharthan et al., 2023). The reinforcement phase enhances load-bearing capacity, stiffness, and wear resistance, while the matrix contributes ductility and toughness wear. The selection of reinforcement is guided by parameters such as morphology, size, density, melting point, hardness, and elastic modulus (Beldar and Kadbhane, 2025; Chenrayan et al., 2023; Eisay and Turan, 2025; Liu et al., 2025; Morampudi et al., 2022; Rajan et al., 2025). Among various MMCs, particulate-reinforced systems are particularly attractive due to their isotropic properties, cost-effectiveness, and ease of processing. Reinforcements such as carbides, oxides, borides, and nitrides have been extensively studied for their ability to enhance strength, hardness, and thermal stability. The choice of matrix material is equally critical; magnesium and its alloys are often preferred for lightweight applications due to their low density, high thermal conductivity, and excellent castability (Cuao-Moreu et al., 2020; Kanca, 2022). The synthesis of MMCs requires precise control of processing parameters to ensure uniform dispersion and strong interfacial bonding between the matrix and reinforcement. The resulting composites offer a tailored balance of mechanical properties, making them ideal candidates for next-generation, energy-efficient structural materials.

In the last few years, considerable efforts have been put into enhancing the wear resistance properties of magnesium-based materials for application in the automobile and aerospace industries. Literature shows that the addition of ceramic reinforcement into the metallic matrix enhances the mechanical and tribological properties of the material (Ashok Kumar and Murugan, 2014; Niraj et al., 2018; Turan et al., 2020). However, the addition of ceramic reinforcement reduces the ductility of the material. In some cases, instead of ceramic particulates, reinforcements like graphite and boron nitride (BN) are added to the metallic matrix, which acts as a solid lubricant. The addition of such reinforcements decreases the coefficient of friction and enhances the wear resistance properties of the material (Al-maamari et al., 2019; Kaviti et al., 2018). In MMCs, the presence of ceramic reinforcements acts as a resistance to plastic deformation, which ultimately reduces the wear rate. Previous studies on the wear behaviour of MMCs infer that resistance to wear increases with an increase in reinforcement content. In addition, wettability at the reinforcement-matrix interface plays a vital role in determining the wear resistance properties of the materials. Magnesium-based composites exhibit better wettability than other lightweight structural materials like aluminium (Thakur and Dhindaw, 2001). The wear behaviour of the materials is affected mainly by the normal load applied, sliding distance, sliding speed, and reinforcement content. The effect of lubricants and heat generated during the wear test has a significant impact on the tribological behaviour of the materials. Pin-on-disc wear testing setup is generally used to study the wear behaviour of the materials.

Friction stir processing (FSP) is a solid-state technique widely employed to enhance surface and mechanical properties of MMCs. In this method, reinforcement powders are embedded into pre-machined grooves or holes on the matrix surface, followed by stirring with a rotating tool. The severe plastic deformation induced by the tool promotes dynamic recrystallisation, grain refinement, and uniform dispersion of reinforcements, thereby improving hardness, strength, and wear resistance (Biradar et al., 2025; Aval and Galvão, 2024; Shao et al., 2024). Faraji and Asadi, 2011 demonstrated the synthesis of AZ91/Al_2O_3 composites via FSP, highlighting the influence of tool geometry, rotational speed, and traverse rate on microstructural refinement and mechanical enhancement. Optimal conditions (900 rpm, 40 mm/min, square pin) yielded a refined surface layer with improved properties. Similarly, Vedabouriswaran and Aravindan, 2018 developed RZ5-based composites reinforced with B_4C, MWCNTs, and ZrO_2–Al_2O_3 mixtures, achieving grain sizes of 0.8–1.87 μm in the stir zone compared to 81 μm in the base material, with hardness increasing from 81 HV to 293–403 HV. Advanced approaches combining FSP with high-energy ball milling (HEBM) have further refined grain structures. Liao et al., 2017 reported significant grain reduction in Mg-Gd-BN composites, with particle-stimulated nucleation yielding grain sizes of 3.5 μm in the powder zone versus 8.2 μm in the stir zone. Arokiasamy and Ronald, 2017 observed grain refinement from 84 μm to 7 μm and hardness improvement from 59.3 HV to 69.7 HV in Mg-SiC-Al_2O_3 hybrid composites, attributing enhancements to multi-pass FSP and the pinning effect of reinforcements. These studies affirm FSP as a versatile and effective method for tailoring the microstructure and enhancing the tribo-mechanical performance of magnesium-based MMCs.

Previous studies have demonstrated that the FSP significantly enhances the surface properties of Al7570 alloys through the incorporation of various reinforcing particles, including titanium carbide, graphite, silicon carbide, carbon and fly ash (Patil et al., 2019; Patil et al., 2021). The addition of hard or soft ceramic particulates improves mechanical performance, while solid lubricants reduce wear and friction. Sharma et al., 2019 reported that Al6061 composites reinforced with SiC and graphene nanoplatelets (GNPs) exhibited a 34% reduction in the coefficient of friction and a 50% decrease in specific wear rate compared to the base alloy. Tokunaga et al., 2008 achieved a Vickers microhardness of ~120 HV and tensile strength exceeding 253 MPa in Al-based composites reinforced with fullerene (C_{60}/C_{70}), along with a refined grain size of ~80 nm. Naeem, 2017 investigated the dispersion of ball-milled Ni, Al, Zn, Cu, and Mg into Al7570, revealing that Ni addition promoted Al-Ni intermetallic formation, increased dislocation density, and improved hardness. Azadi et al., 2017 highlighted the role of MoS_2 as a soft solid lubricant in Al7075/TiC/MoS_2 hybrids, which enhanced wear resistance but reduced hardness due to the presence of MoS_2. However, the influence of precipitate dissolution on microhardness degradation remains unaddressed. This study aims to investigate the optimization of FSP parameters for integrating hybrid TiO_2/carbon reinforcements to enhance the tribological performance of Al 7xxx series alloys.

Some authors have shown that a hard material is considered as a useful and economical way to improve the performance of components subjected to severe abrasive wear conditions, with a wide range of fill materials (Vencl et al., 2013). It was investigated and compared the abrasion resistance of three different hard coatings (two based on iron and one WC-based), which were intended to be used to repair the impact plates of the ventilation system of the mill. Abrasive wear tests have been carried out using a scratch tester in dry conditions. Three normal loads of 10, 50 and 100 N were used, and a constant sliding speed of 4 mm/s. Scratching was chosen as a relatively light and fast testing method. The wear mechanism analysis showed a significant

influence of the hard coating structure, which together with the hardness, determined the abrasion resistance of the coating.

Abrasion resistance is a very complex response of a material in a tribo-system involving many variables (Mutton and Watson, 1978). In addition to the testing conditions, the abrasion resistance can be correlated with different mechanical properties of the metallic structure, and ultimately with the microstructural development during the process. At first approximation, the hardness is used predominantly as an indicator for enhancing the abrasion resistance of steels, as a result of the general hypothesis that there is a monotonous relationship between abrasion resistance and material hardness. Evolution of the microstructure of a material at and beneath the worn surface differs from the initial microstructure due to the plastic deformation and local work hardening. During the equilibrium state of the real abrasion process, the work hardening of the layer under the surface subjected to abrasive wear (Xu et al., 2016). This evolution of the local mechanical properties and changes in deterioration mechanisms in the area exposed to abrasive attack is seen as one of the main obstacles to build a general and quantitative model for abrasion speed depending on the mechanical properties of the exposed material.

Despite extensive research on reinforced-based metal matrix composites, challenges remain in achieving an optimal balance between mechanical strength, wear resistance and ductility. Conventional ceramic reinforcements enhance tribological performance but often compromise ductility. Moreover, the uniform dispersion of reinforcements and grain refinement at the surface remains a critical issue, particularly in high-performance applications. The FSP has emerged as a promising technique to address these limitations by enabling localized microstructural modification and reinforcement integration. However, the influence of process parameters, reinforcement type, and hybridization strategies on the tribo-mechanical behaviour of reinforced-MMCs requires further investigation. This study aims to develop and characterize TiO_2-based composites reinforced via FSP, focusing on optimizing process parameters and reinforcement combinations to enhance hardness, wear resistance, and microstructural uniformity. The primary goal of this research is to enhance the surface properties of 7075 aluminium alloys using the FSP. The research investigates the effects of traverse rate on the tribological properties of these alloys by varying the incorporation of titanium dioxide (TiO_2) nanoparticles as reinforcements. The objective is to establish a processing–structure–property relationship that supports the design of lightweight, high-performance materials for automotive and aerospace applications.

2.0 EXPERIMENTAL PROCEDURE

The mechanical performance of TiO_2-reinforced metal matrix composites (TiO_2–MMCs) is influenced by key parameters, including spindle speed, traverse speed, volume fraction of reinforcement, and the intrinsic properties of both matrix and reinforcement. A critical factor is the reinforcement–matrix interface, where strong interfacial bonding enhances crack resistance and impedes plastic deformation.

2.1 Material Preparation

Aluminium alloy Al7570 was employed as the base/matrix material, and AISI H13 steel or equivalent was used as the FSP tool. Titanium dioxide (TiO_2) was used as reinforcement for substrates. The dimensions of the reinforcements were validated through image acquisition using scanning electron microscopy (SEM), as illustrated in Figure 1. The particles are considered to

provide a hardening and lubricating effect on the matrix to enhance the tribological properties. Preliminary study on the effect of individual particles will be performed by varying volume percentages (vol%: 4%, 8%, 12%) of the incorporated particles within the aluminium matrix. Al7075 aluminium alloy, procured from Skidtech Engineering Sdn. Bhd., Melaka, Malaysia, was selected as the matrix material. TiO_2 powder (<5 μm, 99% purity) was sourced from Sigma Aldrich, Japan. Before reinforcement application, Al7075 samples were cleaned using acetone (99.0%–99.4% purity) to ensure optimal surface conditions. A full factorial design of experiments (DoE), as outlined in Table 1, is employed to investigate the influence of independent variables – namely, TiO_2 volume fraction and FSP travers speed – on the hardness, friction coefficient and wear rate of Al/TiO_2 composites. Analysis of variance (ANOVA) is conducted to identify statistically significant parameters affecting tribological and mechanical performance. Additionally, process optimization is performed to determine the optimal combination of FSP parameters and hybrid reinforcement ratios for achieving enhanced durability and reduced weight in Al7075 series alloys.

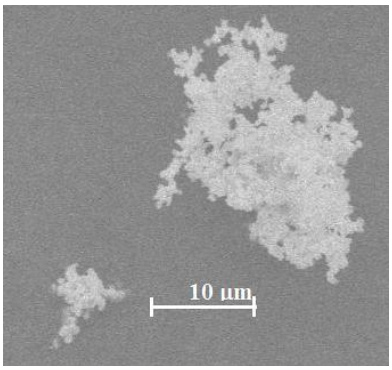

Figure 1: SEM image of nano-sized titanium oxide (TiO_2) particles.

Table 1: Design of experiment.

Std order	Run order	Percentage (vol.%)	Holes no.	Spindle traverse (mm/min)
1	1	2	7	15
2	2	4	13	15
3	3	12	19	15
4	4	2	7	30
5	5	4	13	30
6	6	12	19	30
7	7	2	7	45
8	8	4	13	45
9	9	12	19	45
10	10	0	0	30

2.2 Composite Fabrication

Friction stir welding (FSW) was employed to fabricate the composites. Two sets of formulations were prepared by varying spindle tool speeds and TiO_2 volume fractions. The fabrication of Al-MMC samples via friction stir processing (FSP) is schematically illustrated in Figure 2. Aluminium 7075 base plates were sectioned to dimensions of 100 mm × 100 mm × 10

mm. Arrays of blind holes (2 mm radius, 4 mm depth, spaced 20 mm apart) were machined to accommodate the reinforcing powders and to control the volume fraction of reinforcement, and then the Acetone was applied to ensure they were cleaned. A compacting tool was used to ensure uniform filling of the powders into the blind holes. FSP was conducted using a friction stir welding machine, with a constant tool rotational speed of 1,300 rpm (Ashok Kumar and Murugan, 2014) and varying traverse speeds between 15 and 45 mm/min. A preliminary investigation was carried out using single reinforcements (TiO_2 or carbon) at volume fractions ranging from 2% to 12%. Subsequent experiments examined the effect of hybrid TiO_2/carbon reinforcements at different ratios to evaluate their influence on the composite's tribological and mechanical properties.

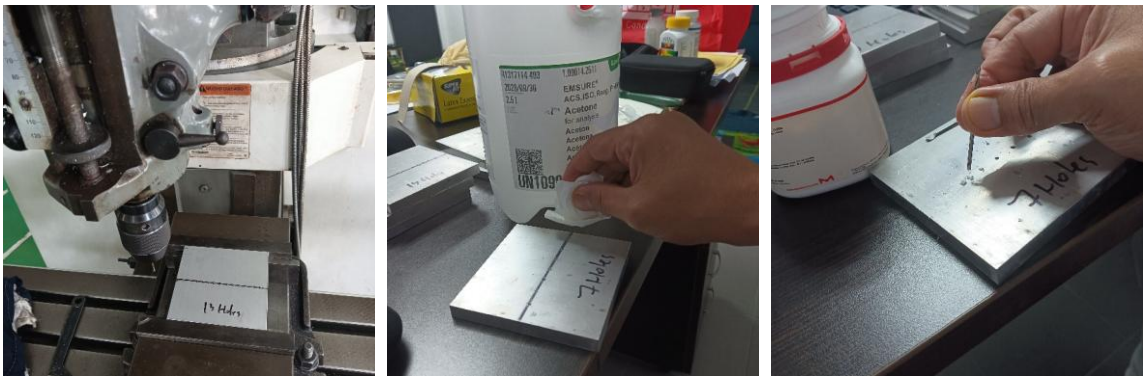

(a) (b) (c)

Figure 2: Schematic representation of the deposition method and TiO_2 volume percentage. (a) drilling process; (b) acetone for the cleaning process; (c) TiO2 particle applied.

2.3 Hardness Evaluation

Hardness measurements were performed following ASTM E18 using a Mitutoyo Rockwell hardness testing machine indentation tester. A load of 500 gf was applied with a dwell time of 10 s. Five indentations were made across the stir zone surface of each FSP specimen, and the average Vickers hardness value was used for subsequent analysis.

2.4 Friction and Wear Evaluation

The friction and wear behaviour of the Al-MMC samples was assessed using the Pin-on-Disk method following ASTM G99. Cylindrical pin specimens (Ø6 mm × 10 mm) were extracted from the FSP zone via EDM wire cutting, while a hardened steel disk (Ø50 mm × 6 mm) served as the counterface. Tests were conducted under varying loads (10–25 N) and rotational speeds (200–1,500 rpm) for 12 minutes. The wear rate was calculated by evaluating the weight measurements taken before and after treatment, expressed as a function of time (g/min). This method provides a thorough and precise assessment of material degradation.

$$W = \frac{W_1 - W_2}{t} \tag{1}$$

where W_1 and W_2 are the initial and final masses of the pin, respectively, and t is the test duration

2.5 Metallography and Surface Morphology

To investigate the microstructural evolution induced by FSP, metallographic analysis was conducted using optical microscopy. Specimens (6 mm × 6 mm × 6 mm) were sectioned from the stir zone via EDM wire cutting and mounted in resin. Samples were ground using 1200# and 2400# SiC papers, followed by diamond polishing and etching with Flick's reagent (90–100 mL H_2O and 0.1–10 mL HF) to reveal grain boundaries. Surface morphology and wear mechanisms were further examined using a Thermo Scientific scanning electron microscope (SEM).

3.0 RESULTS AND DISCUSSION

3.1 Microstructural Analysis

Microstructural analysis was conducted on Al7075–TiO_2 surface composites with contrasting wear performance: specimen no. 5 (minimum wear rate) and specimen no. 2 (maximum wear rate). Optical microscopy, SEM, and elemental mapping analysis were used to characterize the stir zone. Figure 3 illustrate TiO_2 distribution within the stir zones, which shows encapsulated TiO_2 particles in specimen no. 7, indicating zones of uniform dispersion, dense clustering, and particle-free regions influenced by material flow during FSP.

Tool rotational speed significantly affected precipitate morphology, TiO_2 fragmentation, and particle dispersion. Specimen no. 9 (1300 rpm, 45 mm/min) exhibited superior interfacial bonding and partial fragmentation of TiO_2 particles, as shown in Figure 4, compared to the lower TiO_2 filling base alloy (Figure 5). In contrast, specimen no. 1 (1300 rpm, 15 mm/min) showed extensive precipitate dissolution and matrix degradation due to intense plasticization, resulting in weaker bonding and increased surface defects.

TiO_2 were exfoliated in both composites due to shear forces and distributed around the Aluminium sample, forming layers. Although specimen no. 2 demonstrated more uniform particle dispersion due to lower reinforcement volume and higher stirring intensity, it also exhibited more pronounced surface cracks and porosity. These findings suggest that moderate FSP parameters favour improved microstructural integrity and wear resistance, while excessive stirring compromises matrix strength. The FESEM investigation revealed strikingly similar results in the heat-treated alloy discussed in document order no. 2 than in order no. 7, reinforcing the significance of these findings (Santos et al., 2018). Microstructural analysis was conducted on Al7075–TiO_2 surface composites with contrasting wear performance: specimen no. 5 (minimum wear rate) and specimen no. 2 (maximum wear rate). Optical microscopy, SEM, and elemental mapping analysis were used to characterize the stir zone. Figures 3 to 5 illustrates TiO_2 distribution within the stir zones, revealing encapsulated TiO_2 particles in specimen no 7 and variations in dispersion quality. In specimen no. 2, TiO_2 particles appeared more evenly distributed across the stir zone, with fewer large agglomerates and reduced particle-free regions, indicating comparatively uniform dispersion. In contrast, specimens processed at lower traverse speeds exhibited more evident clustering and void formation. It should be noted that this assessment of dispersion uniformity was performed qualitatively, based on SEM micrographs and elemental mapping comparisons, without applying formal statistical clustering analysis. Future work will incorporate quantitative image-processing methods (e.g., particle size distribution and spatial dispersion indices) to validate dispersion uniformity.

Specimen No. 9, processed at a rotational speed of 1300 rpm and a traverse speed of 45 mm/min, exhibited outstanding wear performance. This configuration effectively achieved an

optimal balance between shear and thermal conditions, facilitating partial fragmentation and uniform dispersion of TiO_2 while preventing excessive softening of the matrix material. By maintaining a fixed rotational speed of 1300 rpm and increasing the traverse speed to 45 mm/min, the tool's dwell time per unit length is reduced. This reduction helps to limit local overheating, thereby mitigating extensive dissolution of precipitates and thermal softening of the Al7075 matrix, which in turn preserves interfacial strength. Moreover, the high stirring and shear rates resulting from the tool motion at this traverse speed generate sufficient mechanical energy to partially break up TiO_2 agglomerates into finer fragments, ensuring their even distribution throughout the stir zone. The finer, well-dispersed TiO_2 fragments enhance the load-bearing capacity, promote effective mechanical interlocking between the particles and the matrix, and reduce stress concentrations that could lead to particle pull-out and delamination. Collectively, these factors contribute to lower wear rates and improved hardness. The observed characteristics of superior interfacial bonding and partial fragmentation of TiO_2 in Run 9 align with the findings presented in the accompanying SEM analysis shown in Figure 4.

3.2 Wear Mechanisms

Scanning electron microscopy (SEM) was employed to investigate the wear mechanisms of the base Al7075 alloy and TiO_2-reinforced surface composites. As illustrated in Figure 6, the worn surface of the base alloy demonstrates evident wear characteristics, suggestive of adhesive failure mechanisms. During the process of wet sliding against a mild steel disc, repeated asperity contacts led to localized plastic deformation, as well as the initiation and propagation of cracks. The observation of oxide debris and fragmented particles further substantiates the occurrence of fretting-induced damage and soft matrix adhesion (Patil et al., 2021).

In contrast, the surface composites demonstrated dominant wear mechanisms of abrasion and delamination. Figure 7 reveal ploughing marks, surface wear pattern and reduced fretting behaviour due to the encapsulation of TiO_2 particles. The hard TiO_2 particles contributed to abrasive wear, forming parallel grooves, mitigating surface damage. This figure shows that specimen no. 2 exhibited more severe delamination and crater formation compared to specimen no. 5, attributed to matrix weakening from excessive precipitate dissolution at higher rotational speeds. Although particle dispersion was more uniform in specimen no. 2, the compromised matrix integrity led to increased reinforcement detachment and deeper wear tracks. These observations confirm a transition in wear mechanisms from adhesion and fatigue in the base alloy to abrasion and delamination in the composites, with wear resistance strongly influenced by interfacial bonding and processing parameters.

Figure 3: SEM micrograph captured at 1,000× magnification, revealing clusters of TiO_2 particles within the stir zone of Run 7.

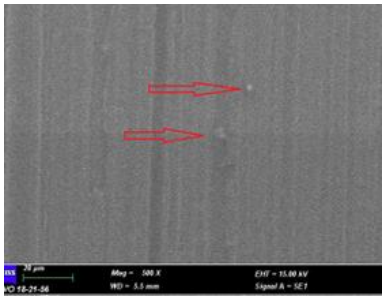

Figure 4: SEM micrograph captured at 500× magnification, revealing clusters of TiO_2 particles within the stir zone of Run 9.

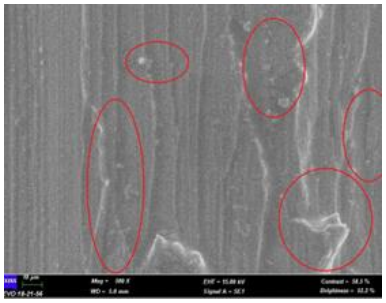

Figure 5: SEM micrograph captured at 500× magnification, revealing clusters of TiO_2 particles within the stir zone of Run 2.

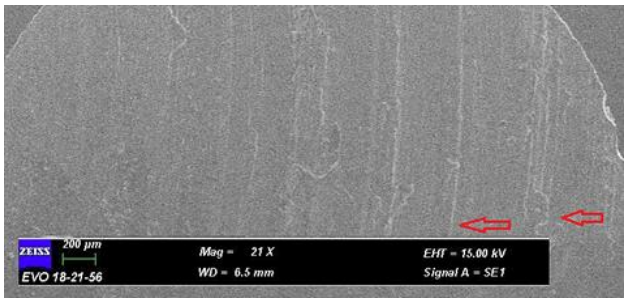

Figure 6: SEM micrograph of wear debris obtained from the Al7075–TiO_2 composite sample in Run 2.

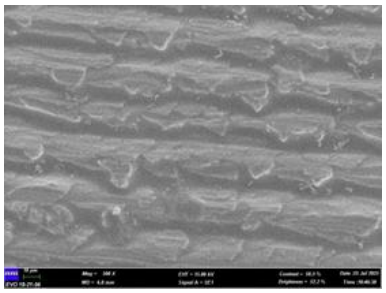

Figure 7: Wear debris obtained from the Al7075–TiO_2 composite sample in Run 2.

The relationship between titanium TiO_2 content (%), traverse speed and the wear performance of Al7075–TiO_2 composites is presented in Table 2. At lower reinforcement levels of 4% and 8% TiO_2, the weight loss rate remains constant at 0.001 g/min across all traverse speeds. This observation indicates that traverse speed has a negligible impact on wear resistance in these compositions. Conversely, the composite containing 12% TiO_2 demonstrates a significant enhancement in wear resistance, as evidenced by a reduction in weight loss rate to 0 g/min at traverse speeds of 15 mm/min and above. This improvement can be attributed to superior particle distribution and an increased load-bearing capacity associated with higher TiO_2 content.

Furthermore, the effect of traverse speed becomes increasingly pronounced at elevated reinforcement levels. The increased speeds facilitate improved microstructural refinement and enhanced dispersion of TiO_2 particles, resulting in diminished material loss during wear testing. These findings suggest that elevating TiO_2 content to 12% markedly improves the wear resistance of Al7075 composites, particularly when processed at moderate to high traverse speeds. This enhancement is likely due to improved load transfer, reduced matrix softening and stronger bonding between the particles and the matrix.

Table 2: Wear performance of Al7075–TiO_2 composites.

Ti (%)	Traverse speed (mm/min)	Weight B (g)	Weight A (g)	Weight (g)/min
4	0	0.37	0.36	0.001
	15	0.37	0.36	0.001
	30	0.36	0.35	0.001
	45	0.35	0.34	0.001
8	0	0.37	0.36	0.001
	15	0.36	0.35	0.001
	30	0.35	0.34	0.001
	45	0.37	0.36	0.001
	0	0.37	0.36	0.001
12	15	0.36	0.36	0
	30	0.33	0.33	0
	45	0.35	0.35	0

3.3 Hardness Evaluation

The Rockwell hardness test was conducted on specimens with finely polished surfaces to ensure accurate indentation measurements. The Rockwell hardness (HRB) measurements of the Al7075–TiO_2 composite at varying traverse speeds are summarized in Figure 8. Figure 8 summarizes the hardness values of the Al7075 alloy reinforced with TiO2 across different weight percentage compositions. The results, as depicted in the Figure, indicate that the composite containing 12 vol.% TiO2 exhibited the highest hardness among the tested samples. Interestingly, a lower TiO_2 content below 12 vol.% led to a reduction in hardness. The increase in hardness may enhance the ability of the composite. The results indicate a relatively stable hardness response across the tested speeds, with values ranging from 84.3 to 86.8 HRB. At 0 mm/min, the hardness was recorded at 85 HRB, slightly decreasing to 84.3 HRB at 30 mm/min. Interestingly, a notable increase to 86.8 HRB was observed at 45 mm/min, suggesting that higher traverse speeds may

contribute to enhanced surface hardening, potentially due to improved particle distribution and thermal effects during processing. These findings highlight the influence of processing parameters on the mechanical integrity of the composite material.

The Rockwell hardness (HRB) values comparison of the 8 vol.% TiO_2 composites at varying traverse speeds is presented in Figure 9. At a traverse speed of 0 mm/min, the material exhibited the highest hardness of 85 HRB. However, a significant reduction in hardness was observed at 15 mm/min, dropping to 71 HRB. As the traverse speed increased to 30 mm/min and 45 mm/min, the hardness values slightly recovered to 74 HRB and 74.5 HRB, respectively. This trend suggests that lower traverse speeds may promote better consolidation and particle bonding, resulting in higher hardness. Conversely, intermediate speeds may introduce thermal softening or microstructural changes that reduce hardness. The partial recovery at higher speeds could be attributed to improved stirring action and refinement of the microstructure. Overall, the data indicate that traverse speed plays a critical role in influencing the hardness characteristics of the composite. In contrast, intermediate speeds likely introduce thermal softening and microstructural instability, which reduce hardness – a phenomenon consistent with thermal effects observed in FSP studies (Tokunaga et al., 2008; Faraji and Asadi, 2011). The recovery at higher speeds may be attributed to improved stirring action and grain refinement, reinforcing the role of processing parameters in determining the mechanical integrity of the composite.

The observed enhancement in wear resistance at higher traverse speeds, particularly in specimen number 9, can be attributed to improved fragmentation and dispersion of TiO_2, as well as the effective preservation of the alloy's strengthening precipitates. Although the nanoscale precipitates are not directly visible in the SEM images, their retention is inferred from the increased hardness and reduced matrix softening noted at these speeds. This interpretation is consistent with findings from Santos et al., 2018, which demonstrated that controlled thermal input during friction stir processing (FSP) helps mitigate the dissolution of precipitates. Future investigations will employ higher-resolution techniques such as transmission electron microscopy (TEM) or X-ray diffraction (XRD) to directly verify the stability of these precipitates.

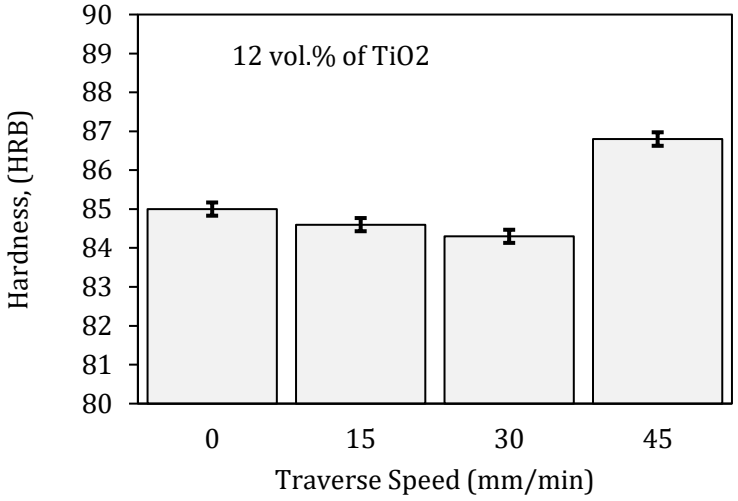

Figure 8: Hardness test of Al7075 at 12 vol. of TiO_2 composite.

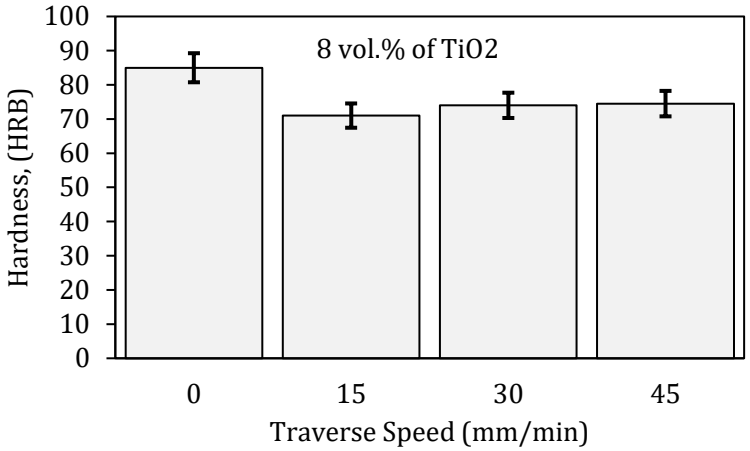

Figure 9: Hardness test of Al7075 at 8 vol. of TiO_2 composite.

The identification of wear mechanisms in this study was conducted through SEM observations of worn surfaces, as well as correlations with the measured wear rates. The base alloy displayed distinct characteristics of adhesive wear, including plastic deformation and the accumulation of oxide debris. In contrast, specimens reinforced with TiO_2 exhibited predominant features of abrasive wear, characterized by grooves and delamination. It is important to highlight that surface profilometry and cross-sectional hardness mapping were not performed in this study. Consequently, the transition from adhesion-dominated to abrasion-dominated wear mechanisms is inferred rather than directly quantified. Future research will incorporate three-dimensional profilometry to accurately assess groove depth and surface roughness, alongside microhardness mapping across the cross-section of the wear track. These enhancements aim to provide quantitative validation of the observed wear transitions.

4.0 CONCLUSION

Al7075–TiO_2 surface composites were successfully fabricated via friction stir processing (FSP), and the influence of processing parameters and reinforcement volume fraction on dry sliding wear behavior was systematically investigated. The key findings are summarized as follows:

(1) The incorporation of TiO_2 particles effectively reduced wear rate by altering dominant wear mechanisms from adhesion to abrasion.
(2) Strong interfacial bonding between TiO_2 particles and the aluminum matrix was identified as a key factor in enhancing wear resistance.
(3) Composites processed under higher traverse speed stirring intensity retained beneficial isomorphous precipitates and exhibited superior wear performance.
(4) Optimal wear resistance was achieved at tool traverse speeds of 45 mm/min, and reinforcement volume fractions of 10–12%.
(5) The composite reinforced with 12 vol.% TiO_2 consistently exhibited superior hardness values, indicating enhanced resistance to deformation due to improved particle reinforcement and distribution.

This study confirms that TiO_2–reinforced Al7075 composites produced by FSP exhibit improved hardness and wear resistance. To further strengthen these findings, future work will incorporate thermal analysis during processing, TEM-based nanoscale characterization, and surface profilometry of wear tracks. In addition, statistical assessment of particle dispersion and evaluation under dynamic and fatigue-prone loading will be undertaken to validate performance in aerospace-relevant environments.

ACKNOWLEDGEMENT

The authors gratefully acknowledge the financial support from Universiti Teknikal Malaysia Melaka (UTeM) provided through the Short-Term Research Grant PJP/2024/FTKM/PERINTIS/SA0033. The provision of research facilities and equipment by UTeM was instrumental in the successful completion of this study.

REFERENCES

Abbasi-Nahr, M., Mirsalehi, S. E., & Mirhosseini, S. S. (2024). Additive manufacturing of AA5083/TiN-diamond hybrid nanocomposite parts via additive friction stir deposition: Metallurgical structure, mechanical, tribological, and electrochemical properties. Journal of Materials Research and Technology, 30, 8187–8208.

Al-maamari, A. E. A., Iqbal, A. A., & Nuruzzaman, D. M. (2019). Wear and mechanical characterization of Mg–Gr self-lubricating composite fabricated by mechanical alloying. Journal of Magnesium and Alloys, 7(2), 283–290.

Arokiasamy, S., & Anand Ronald, B. (2017). Experimental investigations on the enhancement of mechanical properties of magnesium-based hybrid metal matrix composites through friction stir processing. International Journal of Advanced Manufacturing Technology, 93(1–4), 493–503.

Ashok Kumar, B., & Murugan, N. (2014). Optimization of friction stir welding process parameters to maximize tensile strength of stir cast AA6061-T6/AlNp composite. Materials and Design, 57, 383–393.

Azadi, M., Shamanian, M., & Golozar, M. A. (2017). Hardness and wear behavior of Al7075/TiC/MoS2 surface hybrid composite produced by friction stir processing.

Beldar, P., & Kadbhane, S. (2025). Mechanical and wear analysis of AA6061-T6-SiC-TiC-graphite metal matrix composite. Materials Letters, 382.

Biradar, R., Patil, S., M, N., Sharma, P., & Fernandes, F. (2025). Characterization and evaluation of joint properties of friction stir welded AA7075/GNPs joints obtained using square and cylindrical threaded tools. Journal of Materials Research and Technology, 36, 7925–7949.

Chenrayan, V., Vaishnav, V., Shahapurkar, K., Manivannan, C., Tirth, V., Alarifi, I. M., Alamir, M. A., Pruncu, C. I., & Lamberti, L. (2023). Tribological performance of TiB2-graphene Al7075 hybrid composite processed through squeeze casting: At room and high temperature. Tribology International, 185.

Cuao-Moreu, C. A., Alvarez-Vera, M., García-Sánchez, E. O., Maldonado-Cortés, D., Juárez-Hernández, A., & Hernandez-Rodriguez, M. A. L. (2020). Characterization of a duplex coating (boriding + sputter-deposited AlCrON) synthesized on an ASTM F-75 cobalt alloy. Thin Solid Films, 712.

dos Santos, J. F., Staron, P., Fischer, T., Robson, J. D., Kostka, A., Colegrove, P., Wang, H., Hilgert, J., Bergmann, L., Hütsch, L. L., Huber, N., & Schreyer, A. (2018). Understanding precipitate evolution during friction stir welding of Al-Zn-Mg-Cu alloy through in-situ measurement coupled with simulation. Acta Materialia, 148, 163–172.

Eisay, A. M. S., & Turan, M. E. (2025). Effect of reduced graphene oxide (rGO) on wear properties of Al7075 alloy produced via stir casting. Diamond and Related Materials, 151.

Faraji, G., & Asadi, P. (2011). Characterization of AZ91/alumina nanocomposite produced by FSP. Materials Science and Engineering: A, 528(6), 2431–2440.

Jamshidi Aval, H., & Galvão, I. (2024). Characterization of friction stir welded Al-4Cu-Mg alloy / Al-16Si-4Cu-10SiC composite joint. Journal of Advanced Joining Processes, 9.

Kanca, Y. (2022). Microstructural characterization and dry sliding wear behavior of boride layers grown on Invar-36 superalloy. Surface and Coatings Technology, 449.

Kaviti, R. V. P., Jeyasimman, D., Parande, G., Gupta, M., & Narayanasamy, R. (2018). Investigation on dry sliding wear behavior of Mg/BN nanocomposites. Journal of Magnesium and Alloys, 6(3), 263–276.

Liao, H., Chen, J., Peng, L., Han, J., Yi, H., Zheng, F., Wu, Y., & Ding, W. (2017). Fabrication and characterization of magnesium matrix composite processed by combination of friction stir processing and high-energy ball milling. Materials Science and Engineering: A, 683, 207–214.

Liu, A., Chen, N., Liu, P., Zhang, G., Liu, X., Ma, C., & Gao, S. (2025). Exploring the friction and wear characteristics of MAO and MoSe2 tailored micro-pocket interface across wide temperature range. Surface and Coatings Technology, 496.

Morampudi, P., Ramana, V. S. N. V., Bhavani, K., Kishore Reddy, C., & Vikas, K. S. R. (2022). Wear and corrosion behavior of AA6061 metal matrix composites with ilmenite as reinforcement. Materials Today: Proceedings, 52, 1515–1520.

Mutton, P. J., & Watson, J. D. (1978). Some effects of microstructure on the abrasion resistance of metals. Wear, 48(2), 385–398.

Naeem, H. T. (2017). Characterizations particulates of crushed particles (Al-Zn-Mg-Cu-Ni) for fabrication of surface composites Al-alloy using friction stir processing route.

Niraj, N., Pandey, K. M., & Dey, A. (2018). Tribological behaviour of magnesium metal matrix composites reinforced with fly ash cenosphere. In Materials Today: Proceedings (Vol. 5).

Patil, N. A., Pedapati, S. R., Mamat, O. Bin, & Syah Lubis, A. M. H. (2019). Optimization of friction stir process parameters for enhancement in surface properties of Al7075-SiC/Gr hybrid surface composites. Coatings, 9(12).

Patil, N. A., Pedapati, S. R., Mamat, O., & Lubis, A. M. H. S. (2021). Morphological characterization, statistical modeling and wear behavior of AA7075-titanium carbide-graphite surface composites via friction stir processing. Journal of Materials Research and Technology, 11, 2160–2180.

Prasad, D. K., Tiwari, S., Amarnath, M., Chelladurai, H., Vardhaman, B. S. A., Suresh, B., Ramkumar, J., & Gupta, M. K. (2024). Influence of MWCNTs, ZnO, and boric acid nanomaterial blend on the tribological and thermal properties of lithium grease. Tribology International, 192.

Rajan, G., Kumar, A., & Mula, S. (2025). Influence of friction stir processing on wear behavior of nanosized SiC reinforced AA5083 nanocomposites developed by stir casting. Journal of Manufacturing Processes, 141, 1631–1649.

Rehman, A., Das, S., & Dixit, G. (2012). Analysis of stir die cast Al-SiC composite brake drums based on coefficient of friction. Tribology International, 51, 36–41.

Roshan, R., Ganapathi, A., & Bheemappa, S. (2024). Friction and wear behavior of short carbon fibers milled polyphenylene sulfide composites. Jurnal Tribologi, 40.

Shao, Y., Sun, Y., Guo, P., Liu, Q., Shi, J., He, P., Huang, Z., Li, F., & Chen, S. (2024). Thermomechanical behavior and microstructural characteristics of 7055 aluminum alloy during friction stirring welding. Materials Today Communications, 38.

Sharma, A., Narsimhachary, D., Sharma, V. M., Sahoo, B., & Paul, J. (2019). Surface modification of Al6061-SiC surface composite through impregnation of graphene, graphite & carbon nanotubes via FSP: A tribological study. Surface and Coatings Technology, 368, 175–191.

Sidharthan, S., Raajavignesh, G., Nandeeshwaran, R., Radhika, N., Jojith, R., & Jeyaprakash, N. (2023). Mechanical property analysis and tribological response optimization of SiC and MoS2 reinforced hybrid aluminum functionally graded composite through Taguchi's DOE. Journal of Manufacturing Processes, 102, 965–984.

Thakur, S. K., & Dhindaw, K. (2001). The influence of interfacial characteristics between SiCp and Mg/Al metal matrix on wear, coefficient of friction and microhardness. Wear, 247.

Tokunaga, T., Kaneko, K., Sato, K., & Horita, Z. (2008). Microstructure and mechanical properties of aluminum-fullerene composite fabricated by high pressure torsion. Scripta Materialia, 58(9), 735–738.

Turan, M. E., Zengin, H., & Sun, Y. (2020). Dry sliding wear behavior of (MWCNT + GNPs) reinforced AZ91 magnesium matrix hybrid composites. Metals and Materials International, 26(4), 541–550.

Vedabouriswaran, G., & Aravindan, S. (2018). Development and characterization studies on magnesium alloy (RZ 5) surface metal matrix composites through friction stir processing. Journal of Magnesium and Alloys, 6(2), 145–163.

Vencl, A., Gligorijević, B., Katavić, B., Nedić, B., & Džunić, D. (2013). Abrasive wear resistance of the iron-and WC-based hardfaced coatings evaluated with scratch test method. Tribology in Industry, 35(2).

Xu, X., van der Zwaag, S., & Xu, W. (2016). The scratch and abrasive wear behaviour of a tempered martensitic construction steel and its dual phase variants. Wear, 358–359, 80–88.